

On the Complex Chemistry of the Uranyl Ion

V.* The Complexity of Uranyl Sulfate

STEN AHRLAND

*Department of Inorganic and Physical Chemistry, Chemical Institute, University of Lund,
Lund, Sweden*

From his early cryoscopic and conductometric investigations, Dittrich⁵ concluded that uranyl sulfate was incompletely dissociated. Since then however only one attempt has been made to carry out a quantitative investigation of this complex system, *viz.* by Betts and Michels⁶. Unfortunately serious objections must be raised to their investigation.

Betts and Michels use the method of Job⁷ for an extinctionmetric determination of the composition of the complex solution. This method can however not be applied if more than one complex is formed. As it is very difficult to decide with certainty, if this is the case or not, the method has thus a very limited applicability. Moreover those complex systems which have been thoroughly investigated have, as a rule, been shown to involve more than one complex (see *e.g.* Bjerrum⁸, Leden⁹, Fronaeus^{10,11} Sillén¹²). The method of Job may therefore be used only in rare cases, which are, moreover, not easy to indicate. The attempt of Vosburgh and Cooper¹³ to extend this method to systems involving more than one complex is not useful, as their extension is accompanied by a number of limiting conditions which cannot possibly be fulfilled in practice.

The measurements of Betts and Michels are in addition performed in solutions of a $[H^+] = 2C$. These solutions contain the sulfate chiefly as hydrosulfate ions, which are considered not to form any uranyl complexes. The reason given for this opinion⁶ p. S289 is however not conclusive as the same behaviour would be observed if both sulfate and hydrosulfate ions form complexes.

* The preceding papers of this series (Ahrlund¹⁻⁴) are in the following referred to as I–IV. Unless otherwise stated, the symbols in the present paper refer to the same quantities as those mentioned in the previous papers.

In the present investigation the complexity of uranyl sulfate is determined potentiometrically as well as extinctionmetrically.

The potential measurements are performed according to the method of ligand displacement, developed by Fronæus¹¹. This is the only known potentiometric method which is applicable here. A suitable displacing ligand has been found in the acetate ion. As shown in IV, this ion forms strong complexes with the uranyl ion, and the experimental conditions can be chosen so that the hydrolysis of the uranyl ion and its complexes does not interfere with the acetate complex formation.

The extinction measurements are carried out according to the method described in II and IV.

In all the measurements, the ionic medium is built up in the same manner as in I—IV, having a ionic strength = 1 C with NaClO_4 as the supplementary neutral salt. The temperature is 20° C.

Chemicals used: Baker's analyzed *sodium sulfate* is used without further purification. A stock solution with $C_A \approx 1/3$ C is prepared. It is analyzed by a) drying a sample and weighing the residue and b) passing a sample through an ion exchange column saturated with hydrogen ions and then titrating alkalimetrically. Both the methods give $C_A = 334$ mC.

The other chemicals are of the same preparations as in I and IV.

THE POTENTIAL MEASUREMENTS

a. Equations for the calculation of the complexity constants

At measurements made by the method of ligand displacement the solutions contain two competing ligands A and B. Thus the central group M may form complexes with A or B as well as mixed complexes with both A and B. Provided that the complexity of the B-system is stronger than that of the A-system it is then possible to calculate not only the constants of the complexes MA_j ($j = 1, 2, \dots, N$) but also those of the mixed complexes of the type MA_jB ($j = 1, 2 \dots N-1$), by measuring merely the free ligand concentration $[\text{B}]$.

From $[\text{B}]$, the ligand number with respect to B, \bar{n}_B , is calculated. At a given $[\text{B}]$, this quantity is smaller in solutions containing A than in solutions free from A, owing to the competing complex formation between M and A. The difference, $\Delta\bar{n}_B$, will, however, grow smaller and smaller, as $[\text{B}]$ is increased at a constant value of $[\text{A}] = [\text{A}]_0$, and it will cease completely within the random errors at a finite value of $[\text{B}]$, b, if the complexity of the B-system is sufficiently strong. Practically all A-ligands of the complexes are then replaced

by B-ligands. The value of b will depend on the mutual strength of the complex systems, and, of course, on the value of $[A]_n$ chosen.

In order to get $\Delta \bar{n}_B$ for solutions of a constant and known $[A]_n$ it is necessary to make measurements at different C_M and then extrapolate to $C_M = 0$, where $C_A = [A]_n$. By this, the influence of polynuclear complexes is also removed, and the method therefore permits a correct determination of all mononuclear constants even if polynuclear complexes exist.

From the data thus measured the function $X([A]_n)$ is obtained by the equation (Fronaeus ^{11 p.75})

$$\ln X([A]_n) = \int_0^b \left(\frac{\Delta \bar{n}_B}{[B]} \right)_{C_M=0} d[B] \quad (1)$$

The integration is carried out graphically and from $X([A]_n)$ thus found the functions $X_1([A]_n)$, $X_2([A]_n)$ and $X_3([A]_n)$ are formed and the constants β_i of the complexes MA_i calculated in the usual way (II p. 787).

The mixed constants $\beta_{i,1}$ of the complexes MA_iB are then calculated according to (Fronaeus ^{11 p.76}):

$$\lim_{[B] \rightarrow 0} \left(\frac{\bar{n}_B}{[B]} \right)_{C_M=0} = \frac{\sum_{i=0}^{N-1} \beta_{i,1} [A]^i}{X([A])} \quad (2)$$

Here $X([A])$ is known from (1), and $\beta_{0,1}$ is the first constant of the B-system, which is known in advance. The other constants $\beta_{i,1}$ are then calculated according to an extrapolation method analogous to the one employed when the constants β_i are calculated from the X -functions. Thus the function $U_1([A])$ is formed according to

$$U_1([A]) = \frac{X([A]) \cdot \lim_{[B] \rightarrow 0} \left(\frac{\bar{n}_B}{[A]} \right)_{C_M=0} - \beta_{0,1}}{[A]} = \sum_{j=1}^{N-1} \beta_{j,1} [A]^{j-1} \quad (3)$$

The extrapolation of $U_1([A])$ to $[A] = 0$ gives $\beta_{1,1}$. We are then able to form a new function

$$U_2([A]) = \frac{U_1([A]) - \beta_{1,1}}{[A]} = \sum_{j=2}^{N-1} \beta_{j,1} [A]^{j-2} \quad (4)$$

the extrapolation of which to $[A] = 0$ gives $\beta_{2,1}$, etc.

b. The calculation of [B] and \bar{n}_B

The experiments are quite analogous to those of IV. In both cases, the quantities immediately searched for are the free acetate ion concentration (here = [B]) and the ligand number with respect to acetate (here = \bar{n}_B). They are calculated from measurements of $[H^+]$ of an acetate buffer. These measurements are very accurately and conveniently performed by means of the quinhydrone electrode. As stated in IV, the influence of the hydrolysis of the uranyl species can be neglected in a buffer with $C'_{HB}/C'_B = 5.0$. Therefore this buffer is used here. The $[H^+]$ of the solutions then becomes so high however, that the formation of hydrosulfate ions must be taken into consideration, and so the equations of IV have to be accordingly modified when used here.

As in IV, two solutions are compared, the first one (denoted ') containing no uranyl, the second one with the uranyl concentration C_M . The law of mass action then gives the following equation for the dissociation of the acetic acid:

$$\frac{[H^+]' (C'_B + [H^+]' + [HSO_4^-]')}{C'_{HB} - [H^+]' - [HSO_4^-]'} = \frac{[H^+][B]}{C'_{HB} - [H^+] + C_H^o - C_s - [HSO_4^-]} \quad (5)$$

We introduce $C'_{HB} = \delta \cdot C'_B$ and

$$[HSO_4^-] = [H^+][SO_4^{2-}]/K_2 \approx [H^+] \cdot C_A/K_2 \quad (6)$$

As $[HSO_4^-]$ is a correction term, the approximation $[SO_4^{2-}] \approx C_A$ may be permitted. Further, the term C_s is put = 0, according to IV, pp. 203, 205. So we obtain for [B]:

$$[B] = \frac{[H^+]'}{[H^+]} \cdot \frac{(C'_B + [H^+]'(1 + C_A/K_2))(\delta \cdot C'_B - [H^+](1 + C_A/K_2) + C_H^o)}{\delta \cdot C'_B - [H^+](1 + C_A/K_2)} \quad (7)$$

or, approximately, with the value $\delta = 5.0$ inserted:

$$[B] = \frac{[H^+]'}{[H^+]} (C'_B + 1.2 \vartheta' - 0.2 \vartheta + 0.2 C_H^o) \quad (8)$$

if the expressions $[H^+](1 + C_A/K_2)$ and $[H^+]'(1 + C_A/K_2)$ are denoted by ϑ and ϑ' respectively.

For \bar{n}_B we obtain the expression (cf. IV p. 203):

$$\bar{n}_B = \frac{C'_B + [H^+] - C_H^o + C_s + [HSO_4^-] - [B]}{C_M} \quad (9)$$

Table 1. Determination of E' as a function of C'_B at different C'_A . The calculated values of ϑ' ($[H^+]_0 = 10.19$ mC).

$C'_A \rightarrow$ mC	25		50		100		150		200	
C'_B mC	E' mV	ϑ' mC	E' mV	ϑ' mC	E' mV	ϑ' mC	E' mV	ϑ' mC	E' mV	ϑ' mC
10.37	110.4	0.17	110.1	0.21	109.4	0.29	109.1	0.38	108.8	0.47
20.20	110.0	0.17	109.6	0.21	108.8	0.30	108.5	0.39	107.9	0.48
29.55	109.8	0.17	109.4	0.21	108.6	0.30	108.2	0.40	107.5	0.49
38.4	109.7	0.2	109.3	0.2	108.6	0.3	108.0	0.4	107.3	0.5
46.9	109.7	»	109.3	»	108.5	»	107.9	»	107.2	»
66.5	109.6	»	109.2	»	108.4	»	107.7	»	107.0	»
99.7	109.6	»	109.2	»	108.3	»	107.6	»	106.8	»
138.9	109.6	»	109.2	»	108.3	»	107.6	»	106.8	»
177.3	109.6	»	109.2	»	108.3	»	107.6	»	106.7	»
206.0	109.7	»	109.3	»	108.4	»	107.6	»	106.7	»
228.0	109.7	»	109.3	»	108.4	»	107.7	»	106.7	»
260.0			109.5	»	108.6	»	107.8	»	106.8	»

which gives, when simplified according to the above:

$$\bar{n}_B = \frac{C'_B - (C_H^0 - \vartheta) - [B]}{C_M} \quad (10)$$

In these equations of $[B]$ and \bar{n}_B , the quantities $[H^+]', [H^+], C_H^0$ and $[H^+]' / [H^+]$ are calculated exactly as in IV, i.e. from the equations (16), (17) and (18) of II, respectively. It should be noted, that the quantity $E' - E$ ($= E_A$ of II) is called E_B here, as it is the emf caused by the complex formation of the acetate ions (here = B). C'_B , ϑ and C_A are stoichiometrically known. K_2 has been determined by Fronaeus^{11 p.80} to $8.4 \cdot 10^{-2}$ C for the medium and temperature used.

c. Experimental data

The complex solutions are prepared by mixing the solutions (cf. I p. 383):

$$S = \begin{cases} C'_M \text{ mC } \text{UO}_2(\text{ClO}_4)_2 \\ C'_A \text{ mC } \text{Na}_2\text{SO}_4 \\ (1\,000 - 3C'_M - 3C'_A) \text{ mC } \text{NaClO}_4 \end{cases} \quad T = \begin{cases} C'_A \text{ mC } \text{Na}_2\text{SO}_4 \\ 400 \text{ mC } \text{NaAc}^* \\ 2\,000 \text{ mC } \text{HAc} \\ (400 - 3C'_A) \text{ mC } \text{NaClO}_4 \end{cases}$$

* Ac = acetate.

Table 2. Determination of corresponding values of $\bar{n}_B/[B]$ and $[B]$ at different C'_A and C'_M .

			$C'_A = 25 \text{ mC}$				$C'_A = 50 \text{ mC}$			
No	C_M mC	C'_B mC	E_B mV	$C_H^0 - \vartheta$ mC	[B] mC	$\bar{n}_B/[B]$ C ⁻¹	E_B mC	$C_H^0 - \vartheta$ mC	[B] mC	$\bar{n}_B/[B]$ C ⁻¹
$C'_M = 25 \text{ mC}$										
1	24.35	10.37	42.8	0.22	1.93	175	38.3	0.03	2.33	141.5
2	23.75	20.20	41.0	0.24	4.03	166.5	36.6	0.06	4.81	134.5
3	23.15	29.55	39.6	0.25	6.19	161	35.3	0.07	7.36	129.5
4	22.6	38.4	38.1	0.3	8.59	150.5	33.9	0.1	10.12	123.5
5	22.05	46.9	36.0	»	11.35	140.5	32.3	»	13.1	116.5
6	21.55	55.1	33.5	0.4	14.69	127	30.0	0.2	16.85	105
7	20.85	66.5	29.5	»	20.75	105	26.4	»	23.5	87.5
8	19.75	84.0	22.8	0.5	34.2	73	20.9	0.3	36.9	64.5
9	18.75	99.7	17.8	»	49.4	54	16.5	0.4	52.0	48.5
10	17.85	114.0	14.4	»	64.6	42.5	13.8	»	66.2	40
11	17.05	127.0	12.0	»	79.2	35	11.6	»	80.5	33.5
12	16.3	138.9	10.4	»	92.3	30.5	10.0	0.3	93.8	29.5
13	15.0	159.6	8.1	»	116.1	24.5	7.8	»	117.5	24
14	13.9	177.3	6.5	0.4	137.4	20.5	6.3	»	138.3	20
15	12.1	206.0	4.8	»	170.6	17	4.7	0.2	171.4	16.5
16	10.7	228.0	3.9	0.3	195.9	15	3.6	»	198.1	14
17	8.72	260.0								
$C'_M = 50 \text{ mC}$										
18	48.7	10.37	61.6	0.29	0.927	203	57.7	0.04	1.084	175
19	47.5	20.20	58.7	0.42	2.005	186.5	54.6	0.18	2.36	157.5
20	46.3	29.55	57.1	0.46	3.11	180.5	53.1	0.23	3.66	151.5
21	45.2	38.4	55.9	0.5	4.24	176	51.9	0.3	4.96	148
22	44.1	46.9	54.9	»	5.37	173	50.9	»	6.28	145.5
23	43.1	55.1	53.6	»	6.65	167.5	49.5	»	7.80	140
24	41.7	66.5	51.4	0.6	8.73	157	47.4	0.4	10.21	131.5
25	39.5	84.0	47.1	0.7	13.06	136.5	43.2	0.5	15.25	113.5
26	37.5	99.7	41.6	0.8	19.23	110	38.1	0.6	22.3	92
27	35.7	114.0	35.7	0.9	27.85	86	33.0	0.8	31.0	74.5
28	34.1	127.0	30.2	1.0	38.5	67	28.1	»	41.9	59
29	32.6	138.9	25.2	»	51.4	51.5	24.1	»	55.8	45.5
30	30.0	159.6	18.8	»	76.0	36.5	18.3	»	77.3	35
31	27.8	177.3	14.9	»	98.6	28.5	14.6	»	99.8	27.5
32	24.2	206.0	10.6	0.8	135.5	21	10.2	0.7	137.7	20.5
33	21.4	228.0	8.0	0.7	166.3	17	7.9	0.6	167.1	17
34	17.45	260.0								

Table 2 (continued).

No	$C'_A = 100 \text{ mC}$				$C'_A = 150 \text{ mC}$				$C'_A = 200 \text{ mC}$			
	E_B mV	$C_H^0 - \vartheta$ mC	[B] mC	$\bar{n}_B/[B]$ C ⁻¹	E_B mV	$C_H^0 - \vartheta$ mC	[B] mC	$\bar{n}_B/[B]$ C ⁻¹	E_B mV	$C_H^0 - \vartheta$ mC	[B] mC	$\bar{n}_B/[B]$ C ⁻¹
$C_M = 25 \text{ mC}$												
1	32.5	-0.34	2.94	108.5	27.8	-0.61	3.56	85.5	24.5	-0.83	4.07	72
2	31.3	-0.34	5.94	103.5	26.9	-0.62	7.10	81.5	23.5	-0.84	8.13	67
3	30.3	-0.32	9.00	100	26.0	-0.60	10.69	78.5	22.8	-0.83	12.17	65
4	29.3	-0.3	12.14	97	24.9	-0.6	14.49	75	21.9	-0.8	16.29	62.5
5	27.6	»	15.81	90	23.8	-0.5	18.45	71.5	20.8	»	20.75	59
6	25.8	-0.2	20.0	82	22.3	»	22.9	66.5	19.6	-0.7	25.6	55
7	23.2	»	26.7	72	20.0	-0.4	30.3	58	17.8	»	33.1	49.5
8	18.9	-0.1	39.9	56	16.6	»	43.7	47	15.0	-0.6	46.7	41
9	15.6	0.0	54.0	45	13.9	-0.3	57.7	39	12.6	-0.5	60.8	34.5
10	13.1	»	68.1	38	11.9	»	71.5	32	10.9	»	74.3	30.5
11	11.2	»	81.8	32.5	10.3	-0.2	84.7	29.5	9.5	»	87.7	26.5
12	9.9	»	94.2	29	8.8	»	98.4	25.5	8.2	-0.4	100.7	23.5
13	8.0	»	116.4	25	7.4	»	119.4	22.5	6.6	»	123.0	20
14	6.7	»	136.5	21.5	6.0	»	140.3	19	5.6	»	142.6	18
15	5.1	»	168.7	18.5	4.3	»	174.2	15	4.0	»	176.2	14
16	4.0	»	195.0	16	3.5	»	198.6	14	3.1	»	202.3	12
17					2.5	»	236.0	12	2.2	»	238.7	10.5
$C'_M = 50 \text{ mC}$												
18	49.7	-0.51	1.49	130	43.9	-0.96	1.87	104	39.3	-1.30	2.25	86
19	46.8	-0.37	3.21	114	41.5	-0.85	3.96	91	37.2	-1.22	4.71	75
20	45.5	-0.32	4.93	109.5	40.3	-0.81	6.05	87	36.2	-1.20	7.13	71.5
21	44.6	-0.3	6.62	107	39.2	-0.8	8.20	84	35.3	-1.2	9.59	69
22	43.7	»	8.36	105	38.2	-0.7	10.40	81	34.5	-1.1	12.08	67.5
23	42.5	-0.2	10.28	101.5	37.3	»	12.65	79	33.5	»	14.72	65.5
24	40.6	»	13.40	95.5	35.5	-0.6	16.37	74	31.9	-1.0	18.88	62
25	36.7	0.0	19.7	83	32.2	-0.5	23.55	65.5	29.2	-0.9	26.5	56
26	32.5	0.1	27.6	69.5	28.8	-0.3	32.0	57	26.0	-0.7	35.8	48
27	28.7	0.2	36.7	59.5	25.4	-0.2	41.8	48.5	23.2	-0.6	45.7	42
28	24.8	0.3	47.6	49	22.3	-0.1	52.7	41.5	20.6	-0.5	56.5	37
29	21.7	»	59.0	41.5	19.7	»	63.8	36	18.4	-0.4	67.3	33
30	16.8	0.4	82.2	31	15.6	0.0	86.3	28.5	14.8	»	89.1	26.5
31	13.7	»	103.3	25.5	12.8	»	107.2	23.5	12.3	-0.3	109.1	22.5
32	9.6	0.3	141.3	19	9.1	»	144.2	18	9.0	»	144.5	17.5
33	7.6	»	169.0	16.5	7.4	»	170.7	15.5	7.2	»	171.8	15.5
34	5.1	0.2	212.8	12.5	5.0	-0.1	213.8	12.5	5.0	»	213.8	12.5

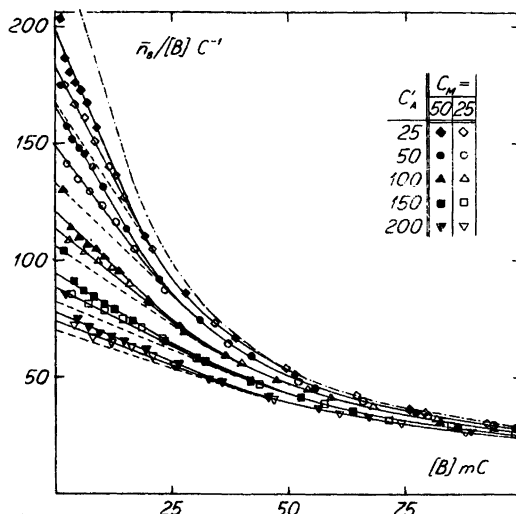


Fig. 1. $\bar{n}_B[B]$ as a function of $[B]$. The curve of dots and dashes refers to pure acetate complex formation (IV Fig. 2). The full-drawn curves are drawn according to the experimental points (scheme on the fig.) The dashed curves give the result of the extrapolations to $C_M = 0$.

Thus, when T is added to S, the resulting solution has always a constant C'_A , while C'_B increases and C'_M decreases. The ionic strength is constant apart from changes owing to the complex formation.

Five different values of C'_A are used viz. $C'_A = 25, 50, 100, 150$ and 200 mC. For every C'_A -series, titrations are performed with $C'_M = 50$ and 25 mC, besides the titration with $C'_M = 0$. The reference electrode, RE, has in the present case $[H^+]_0 = 10.19$ mC.

The titrations of different C'_A with $C'_M = 0$ are collected in Table 1. From the course of E' found, it is plain that an exchange of perchlorate for sulfate implies a greater change of the ionic medium than the corresponding exchange for acetate (cf. IV p. 204).

The main titrations are collected in Table 2. In Fig. 1, $\bar{n}_B/[B]$ is drawn as a function of $[B]$ for the different C'_A and C'_M used. The value of the function for $C_A = 0$ (as determined in IV) is also introduced. The $\bar{n}_B/[B]$ -functions are extrapolated to $[B] = 0$.

At high values of $[B]$, the curves of different C'_M coincide for a given C'_A (Fig. 1). They thus represent the function $(\bar{n}_B/[B])_{C_M=0}$ ultimately searched for (p. 1153). Only at low $[B]$ is it necessary to make an extrapolation. As the difference between the C'_M -curves is relatively slight even there, it is certainly allowed to perform this extrapolation linearly (Table 3). The

Table 3. Determination of $(\bar{n}_B/[B])_{C_M=0}$ as a function of $[B]$ at the different values of $C'_A = C_A = [A]_n$.

	C_M mC	$\bar{n}_B/[B]$ C ⁻¹	C_M mC	$\bar{n}_B/[B]$ C ⁻¹	$\left(\frac{\bar{n}_B}{[B]}\right)_{C_M=0}$	C_M mC	$\bar{n}_B/[B]$ C ⁻¹	C_M mC	$\bar{n}_B/[B]$ C ⁻¹	$\left(\frac{\bar{n}_B}{[B]}\right)_{C_M=0}$
	$C'_M = 50$ mC		$C'_M = 25$ mC		C ⁻¹	$C'_M = 50$ mC		$C'_M = 25$ mC		C ⁻¹
[B] mC	$C'_A = 25$ mC					$C'_A = 50$ mC				
0	50.0	198	25.0	182.5	167	50.0	165	25.0	149	133
5	44.5	174	23.5	163.5	152	45.2	148	23.7	136	122.5
10	41.0	151	22.3	144.5	137	41.8	131.5	22.6	123	113
15	38.9	128	21.5	125.5	122.5	39.6	114	21.8	109.5	104
	$C'_A = 100$ mC									
0	50.0	121	25.0	113.5	601					
5	46.3	111.5	23.95	5.501	99					
10	43.2	102	23.0	98	5.39					
15	41.1	92.5	22.2	89.5	86					
20	39.5	83.5	21.55	81.5	79					
	$C'_A = 150$ mC					$C'_A = 200$ mC				
0	50.0	94.5	25.0	88.5	82.5	50.0	78	25.0	74	70
5	46.9	88.5	24.1	83.5	78	47.35	74	24.25	70.5	66
10	44.3	82.5	23.25	78.5	73.5	45.0	70	23.45	66.5	63
15	42.2	76	22.55	73.5	70.5	42.9	65.5	22.8	63	60.5
20	41.1	70	21.9	68.5	67	41.4	61	22.15	59	57
30	38.0	59.5	20.9	58.5	57.5	38.7	52.5	21.0	51.5	50.5

values of the limes functions $(\bar{n}_B/[B])_{C_M=0}$ thus found are introduced in Fig. 1 as dashed curves.

For these limes functions, we have $[A]_n = C_A$ (cf. above, p. 1153). C_A is connected with C'_A according to $C_A = C'_A - [\text{HSO}_4^-]'$. From Table 1, we are able to calculate the ratio $[\text{HSO}_4^-]'/C'_A \approx [\text{HSO}_4^-]'/[\text{SO}_4^{2-}]' = [\text{H}^+]'/\text{K}_2 \approx 1.5\%$. Thus we may very well neglect $[\text{HSO}_4^-]'$ in comparison with C'_A in the pure buffer, and so put $[A]_n = C_A = C'_A$ for the limes functions.

From Fig. 1, it is now possible to determine the upper limits b of the integration and they are tabulated in Table 4. Unfortunately, these values

Table 4. The X -functions, as obtained by graphical integration according to equ. (1). The ligand number and the composition of the system as calculated from the complexity constants found.

$$\beta_1 = 50 \pm 10 \text{ C}^{-1} \quad \beta_2 = 350 \pm 150 \text{ C}^{-2} \quad \beta_3 = 2\,500 \pm 1000 \text{ C}^{-3}$$

$[A]_n$ mC	b mC	$\ln X([A])$	$X([A])$	$X_1([A])$ C^{-1}	$X_2([A])$ C^{-2}	$X_3([A])$ C^{-3}	\bar{n}_A	α_0 %	α_1 %	α_2 %	α_3 %
0				50	330	2 500					
10							0.38	65	32.5	2.5	0
25	60	0.902	2.465	58.6	340		0.72	40	50	8.5	1.5
50	120	1.575	4.83	76.6	530		1.11	21.5	53.5	18.5	6.5
100	180	2.445	11.53	105.3	550	2 200	1.62	8.5	42	28.5	21
150	240	3.185	24.15	154.3	700	2 500	1.96	4	30	31.5	34.5
200	300	3.815	45.4	222.0	860	2 600	2.18	2	22.5	31	44.5

Table 5. Corresponding values of $[A]_n$, $X([A]_n)$ and $\lim_{[B] \rightarrow 0} \left(\frac{\bar{n}_B}{[B]} \right)_{C_M=0}$. The calculated U -functions and mixed complexity constants.

$$\beta_{1,1} = 6\,000 \pm 1\,500 \text{ C}^{-2} \quad \beta_{2,1} = 40\,000 \pm 15\,000 \text{ C}^{-3}$$

$[A]_n$ mC	$X([A]_n)$	$\lim_{[B] \rightarrow 0} \left(\frac{\bar{n}_B}{[B]} \right)_{C_M=0}$ C^{-1}	$U_1([A])$ C^{-2}	$U_2([A])$ C^{-3}
0		241	6 000	40 000
25	2.465	167	6 800	
50	4.83	133	8 000	40 000
100	11.53	106	9 800	38 000
150	24.15	82.5	11 700	38 000
200	45.4	70	14 700	43 500

cannot be determined with the amount of accuracy which is desired, as the $(\bar{n}_B / [B])_{C_M=0}$ — curves of different $[A]_n$ converge rather slowly. Evidently the complexity of uranyl sulfate is rather strong, and therefore the acetate ions force the sulfate ions out of their complexes only with difficulty. It would have been more advantageous to use a stronger displacing ligand, but, unfortunately, no such stronger ligand is known.

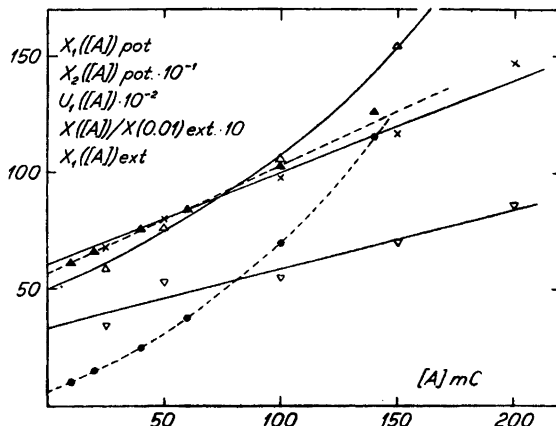


Fig. 2. The functions 1. $X_1([A])$ pot. (Δ), 2. $X_2([A])$ pot. (∇), 3. $U_1([A])$ (\times), 4. $X([A])/X(0.01)$ ext. (\bullet) and 5. $X_1([A])$ ext. (\blacktriangle). The functions found potentiometrically are fulldrawn, those found extinctionimetrically dashed.

With the courses of the functions $(\bar{n}_B/[B])_{C_M=0}$ known, it is possible to perform the graphical integration of (1) using the identity:

$$\int_0^b \left(\frac{\Delta \bar{n}_B}{[B]} \right)_{C_M=0, [A]=[A]_n} \cdot d[B] = \int_0^b \left(\frac{\bar{n}_B}{[B]} \right)_{C_M=0, [A]=0} \cdot d[B] - \int_0^b \left(\frac{\bar{n}_B}{[B]} \right)_{C_M=0, [A]=[A]_n} \cdot d[B] \quad (11)$$

The X -functions hence obtained are found in Table 4 and $X_1([A])$ and $X_2([A])$ are also found in Fig. 2. Their extrapolation to $[A] = 0$ gives β_1 and β_2 . $X_3([A])$ has an almost constant value ($=\beta_3$), thus complexes with more than three ligands cannot be proved within the range of $[A]$ used.

With the constants obtained, \bar{n}_A is calculated ((2) of II) for the values of $[A]_n$ used before, and in addition for $[A] = 10$ mC (Table 4 and fulldrawn

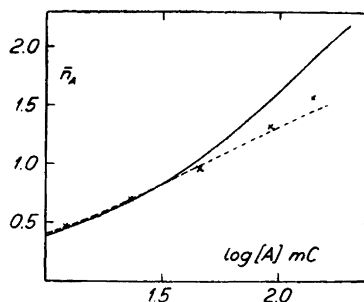


Fig. 3. The complex formation curves. The fulldrawn curve is calculated from the complexity constants found potentiometrically and the dashed one from those found extinctionimetrically. \times = the experimental values of the extinctionimetric investigation (Table 7).

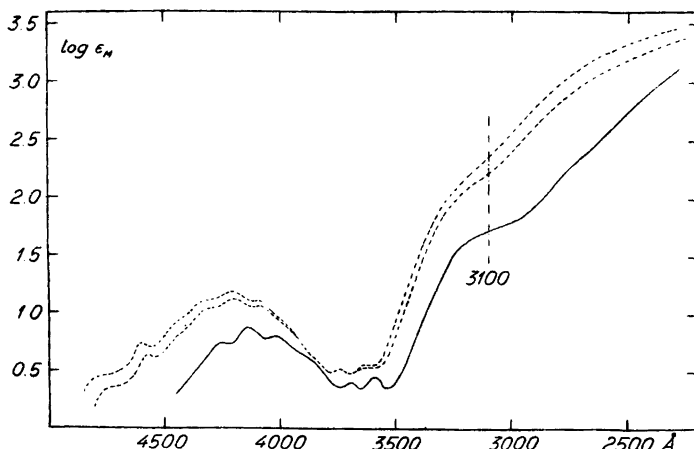


Fig. 4. Extinction curves of a. uranyl ion (full-drawn) and b. complex solutions with $C_M = 10$ mC, $C'_A = 50$ mC (lower dashed) and $C_M = 10$ mC, $C'_A = 200$ mC (upper dashed).

curve of Fig. 3). For the same $[A]$ the composition of the system is also calculated ((8) of II) and given in Table 4.

Then the U -functions are formed according to (3) and (4) and the constants of the mixed complexes MA_iB hence calculated. (Table 5). $U_1([A])$ is also drawn in Fig. 2. Its extrapolation to $[A] = 0$ gives $\beta_{1,1}$. Within the random errors, $U_2([A])$ is a constant ($= \beta_{2,1}$), only the first two complexes MA_iB can thus be proved.

THE EXTINCTION MEASUREMENTS

a. Selection of a wave-length suitable for measurement

To select a suitable wave-length λ , the extinction curves of the following solutions have been measured*:

1. $C_M = 10$ mC, $C'_A = 50$ mC
 2. $C_M = 10$ mC, $C'_A = 200$ mC
- } $I = 1$ by NaClO_4

The curves are found in Fig. 4, together with that of UO_2^{2+} (I p. 377). The extinction of the sulfate and hydrosulfate ions can be neglected in the λ -range used.¹⁵

* As in IV, all extinction measurements are performed with a Beckman Quartz Spectrophotometer DU, improved as described by Adell¹⁴ p. 3.

As seen from the curves, the addition of sulfate causes a considerable change of ϵ_M in different parts of the λ -range. In the visible and near UV regions, however, ϵ_M is so small that very high C_M have to be used to the d :s available. This would imply a not allowed change of the ionic medium. On the other hand, ϵ_M is so great at very short λ that only very low C_M can be used there. But as the present complex system is of medium strength only no marked differences of $[A]$ would then arise between the series of different C_M . Thus no differences would be measured between their ϵ_M either, and the calculation of \bar{n}_A would then be impossible. Thus the middle UV-region must be used, and 3 100 Å is selected as a suitable value of λ .

The solutions are not influenced if kept some days in the dark or in the diffuse day-light (*cf.* II p. 784, 804). The same ϵ_M :s are always found, within the limits of error of the Spectrophotometer.

b. The measurements at $\lambda = 3\,100\text{ Å}$

At $\lambda = 3\,100\text{ Å}$, the hydrolysis of the uranyl ion has a great influence on ϵ_M (*cf.* I 377). Therefore, so much perchloric acid is added to the complex solutions that those of the lowest C'_A acquire a $[H^+] \approx 3\text{ mC}$, the experimental determination of which is performed by quinhydrone electrode using the same RE as above. At this $[H^+]$, the hydrolysis can be neglected even in not complex solutions (I p. 377), while the formation of hydrosulfate is not yet very large. If it is assumed that the slight $[HSO_4^-]$ does not give any appreciable complex formation, (21) of II is valid and may be applied to the determination of $[A]$ and \bar{n}_A in the present system.

Absorption cells of $d = 0.1, 0.3$ and 1 cm are available. As in IV (p. 212), every cell is used in connection with a constant C_M which is chosen so that $C_M \cdot d$ is always a constant, too. At the ϵ_M of the present λ , $C_M = 30, 10$ and 3 mC give suitable values of E . As before, (*cf.* IV p. 212), the differences of transparency between the cells as well as the ratios between their thicknesses are determined by separate measurements.

For every C_M , C'_A has been varied between 10 (or 25) and 300 mC. A further increase of C'_A causes an increase of ϵ_M which is too small to be useful (*cf.* IV p. 216). C'_A lower than those used here would give a very small E , and, moreover, there would be an increase of the influence of that hydrolysis which possibly remains.

The function searched for is $\epsilon_M = f(C_A)$. To find C_A , (14) of II is applied with the simplification $C_s = 0$, *i.e.* the hydrolysis is neglected (*cf.* p. 1154). We thus put $[HSO_4^-] = C'_A - C_A = C_H^0 - [H^+]$. This manner of estimating $[HSO_4^-]$ can be applied here, but not in the potential measurements above

Table 6. ϵ_M as a function of C_A at the different values of C_M .

$C_M \rightarrow$ mC	30		10		3	
$d \rightarrow$ cm	0.1		0.3		1	
C'_A mC	ϵ_M $C^{-1} \cdot \text{cm}^{-1}$	C_A mC	ϵ_M $C^{-1} \cdot \text{cm}^{-1}$	C_A mC	ϵ_M $C^{-1} \cdot \text{cm}^{-1}$	C_A mC
10			87.1	9.8	93.7	9.8
25	102.5	24.7	120.8	24.6	129.0	24.6
50	136.5	49.4	154.8	49.3	161.0	49.3
100	175.1	98.7	187.5	98.8	191.3	98.9
150	195.8	148.2	203.3	148.5	206.0	148.7
200	207.4	197.9	214.2	198.4	216.0	198.5
300	219.9	297.6	224.4	298.1	226.3	298.3

where acetate buffer is present. It gives lower values of $[\text{HSO}_4^-]$ than (6) does, on account of the approximation $[\text{SO}_4^{2-}] \approx C_A$ introduced there. At high C_A , however, where this approximation is a good one, the two methods give much the same result.

The functions $\epsilon_M = f(C_A)$ thus found are tabulated in Table 6, and graphically given in Fig. 5. They are now cut at five constant ϵ_M , the highest value of ϵ_M chosen being $205 \text{ cm}^{-1} \cdot C^{-1}$. Cuts performed at still higher ϵ_M would give too uncertain values of C_A , on account of the slower and slower rise of the ϵ_M -curves. For every ϵ_M chosen, C_A is found to be a linear function of C_M , which indicates a mononuclear complex formation (*cf.* II p. 803). These linear

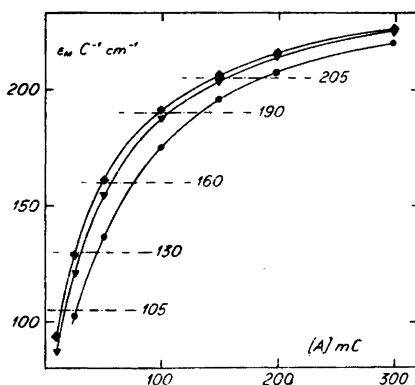


Fig. 5. ϵ_M as a function of C_A at $C_M = 30$ (●), 10 (▼) and 3 mC (•). The curves are cut at five constant ϵ_M , each representing a certain constant value of $[A]$ and \bar{n}_A .

Table 7. C_A as a function of C_M at the selected values of ε_M and the obtained values of $[A]$ and $\bar{n}_A/[A]$.

$C_M \rightarrow$ mC	30	10	3	0		
ε_M $C^{-1} \cdot \text{cm}^{-1}$	C_A mC			$C_A = [A]$ mC	\bar{n}_A	$\bar{n}_A/[A]$ C^{-1}
105	26.3	16.6	13.6	12.1	0.47	39
130	44.2	30.0	25.1	22.9	0.71	31.0
160	74.2	55.1	48.0	45.2	0.97	21.5
190	131.6	105.1	95.6	91.6	1.33	14.5
205	186.0	155.5	144.2	139.6	1.57	11.3

functions have the intercept on the C_A -axis $= [A]$, while their slope gives the corresponding \bar{n}_A . The results are found in Table 7 and Fig. 3.

The X -function are then computed by graphical integration of the $\bar{n}_A/[A]$ -function (Table 8). As no values of $[A]$ are determined in the immediate neighbourhood of the $\bar{n}_A/[A]$ -axis, the integration is performed with $[A]_0 = 10$ mC as the lower limit (*cf.* II p. 786). The integration then gives $X([A])/X(0.01)$. This function, Fig. 2, is extrapolated to $[A] = 0$ and gives $1/X(0.01) = 0.62 \pm 0.03$. Thus $X([A])$ is known, and hence $X_1([A])$ and $X_2([A])$ are formed. The extrapolation of $X_1([A])$ to $[A] = 0$ gives β_1 . Indeed, this function is almost linear within the limited range of $[A]$ available. Thus

Table 8. The X -functions, as obtained by graphical integration of the extinctionmetrically determined $\bar{n}_A/[A]$ -function. The complexity constants and the ligand number obtained from these constants.

$$\beta_1 = 56 \pm 6 \text{ C}^{-1}$$

$$\beta_2 = 450 \pm 50 \text{ C}^{-2}$$

$[A]$ mC	$\ln \frac{X([A])}{X(0.01)}$	$\frac{X([A])}{X(0.01)}$	$X([A])$	$X_1([A])$ C^{-1}	$X_2([A])$ C^{-2}	\bar{n}_A
0		0.62		56.5	465	
10		1.000	1.61	61	450	0.40
20	0.3657	1.441	2.32	66	475	0.64
40	0.9122	2.490	4.01	75.5	475	0.93
60	1.3199	3.743	6.03	84	460	1.10
100	1.9455	7.00	11.3	103	465	1.32
140	2.4481	11.57	18.7	126	495	1.45

$X_2([A])$ is almost a constant $= \beta_2$. Possibly a slight deviation at the highest $[A]$ may be regarded as an indication of the existence of a third complex, but no information can be gained about β_3 .

Ultimately, the difficulty of proving the third complex extinctionsimetrically is certainly due to the circumstance that ϵ_3 has much the same value as ϵ_2 , as can be understood by the course of the ϵ_M -curves at high C_A .

With the constants obtained, \bar{n}_A is calculated according to (2) of II, and given in Fig. 3 as a dashed curve. This curve is seen to fit the experimental points of Table 7 very well, except at the highest $[A]$, where, as said above, the third complex may have some influence.

COMPARISON BETWEEN THE RESULTS OF THE TWO METHODS USED

On comparison between the results gained in potentiometric and extinctionsimetric way, it is seen that the two complex formation curves found coincide at low $[A]$. In harmony with this, consistent values of β_1 and β_2 are obtained according to both methods. At high $[A]$, on the other hand, the curves run apart, the potentiometric curve then being the steepest one. In connection with this, a high value of β_3 is found potentiometrically, whereas it is not possible to determine any value of β_3 extinctionsimetrically.

The discrepancy between the curves is no doubt partly due to the difficulty of determining high $[A]$ extinctionsimetrically, but it is also certain that activity changes are of great importance. From Table 1 it is seen that the exchange of perchlorate for sulfate causes a perceptible change of the medium. It is obvious that this change may affect the two methods in different measure. Moreover, the perchlorate is partly exchanged for acetate buffer in the potentiometric investigation but not in the extinctionsimetric one, and this may also have some influence even if it is not very large to judge from the results of IV p. 204.

SUMMARY

The complexity of uranyl sulfate is investigated potentiometrically as well as extinctionsimetrically. The measurements are performed at 20° C, and the ionic strength is kept $= 1$ C by addition of sodium perchlorate.

The potentiometric investigation is carried out according to the method of ligand displacement¹¹, with acetate as the displacing ligand B. As a buffer of acetate is used, $[B]$ can be determined by measurements of $[H^+]$, carried out by quinhydrone electrode. The acidity of the buffer is chosen so that the hydrolysis of the uranyl species may be neglected. The constants β of the

sulfate complexes MA_j as well as the constants $\beta_{j,1}$ of the mixed complexes MA_jB are computed:

$$\begin{aligned}\beta_1 &= 50 \pm 10 \text{ C}^{-1} & \beta_2 &= 350 \pm 150 \text{ C}^{-2} & \beta_3 &= 2\,500 \pm 1\,000 \text{ C}^{-3} \\ \beta_{1,1} &= 6\,000 \pm 1\,500 \text{ C}^{-2} & \beta_{2,1} &= 40\,000 \pm 15\,000 \text{ C}^{-3}\end{aligned}$$

The extinctionimetric investigation is performed according to the method previously used by the author ^{2,4}. From a study of the extinction curves of uranyl sulfate solutions, 3 100 Å is found to be a convenient wave-length for the main measurements. Perchloric acid is added in sufficient large amounts to suppress the hydrolysis while $[\text{HSO}_4^-]$ is still low. The first two constants β_j can be computed:

$$\beta_1 = 56 \pm 6 \text{ C}^{-1} \qquad \beta_2 = 450 \pm 50 \text{ C}^{-2}$$

A value of β_3 cannot be calculated, but the measurements indicate a value much lower than that of the potentiometric investigation. This may be due partly to the experimental difficulties, partly to activity effects.

On the whole, however, the agreement between the methods employed is good. This proves, firstly that the potentiometric method works well and, secondly that the extinctionimetric method gives the right result, which in turn, implies that the complex formation really is mononuclear.

My thanks are due to Försvarets Forskningsanstalt (FOA), Stockholm, which has given this work a liberal financial support.

REFERENCES

1. Åhrland, S. *Acta Chem. Scand.* **3** (1949) 374 (= I).
2. Åhrland, S. *Acta Chem. Scand.* **3** (1949) 783 (= II).
3. Åhrland, S. *Acta Chem. Scand.* **3** (1949) 1067 (= III).
4. Åhrland, S. *Acta Chem. Scand.* **5** (1951) 199 (= IV).
5. Dittrich, C. *Z. physik. Chem.* **29** (1899) 449.
6. Betts, R. H. and Michels, R. K. *J. Chem. Soc.* (1949), Supplementary issue 286.
7. Job, P. *Ann. chim.* (10) **9** (1928) 113.
8. Bjerrum, J. Diss. Copenhagen (1941).
9. Leden, I. Diss. Lund 1943, *Z. physik. Chem.* **A 188** (1941) 160.
10. Fronaeus, S. Diss. Lund 1948.
11. Fronaeus, S. *Acta Chem. Scand.* **4** (1950) 72.
12. Sillén, L. G. *Acta Chem. Scand.* **3** (1949) 539.
13. Vosburgh, W. C. and Cooper, G. R. *J. Am. Chem. Soc.* **63** (1941) 437.
14. Adell, B. *Acta Chem. Scand.* **4** (1950) 1.
15. Ley, H. and Arends, B. *Z. physik. Chem.* **B 15** (1932) 311.

Received April 19, 1951.